Geographical Analysis
An International Journal of Theoretical Geography

ORIGINAL ARTICLE

Exploring Space-Time Interactions in Fatal Opioid Overdoses

Sergio J. Rey[1] | Elijah Knaap[1] | Alejandra Cabral[2] | Jennifer Syvertsen[3]

[1]Center for Open Geographical Science, San Diego State University, San Diego, California, USA | [2]Department of Community Health Sciences, University of California, Los Angeles, California, USA | [3]Department of Anthropology, University of California, Riverside, California, USA

Correspondence: Sergio J. Rey (srey@sdsu.edu)

Received: 5 August 2024 | **Revised:** 5 March 2025 | **Accepted:** 18 June 2025

Funding: This work was supported by the National Institutes of Health (Grant No. 1R21DA054611-01).

Keywords: harm reduction strategies | opioid overdose cluster | space-time analysis | spatial epidemiology

ABSTRACT

This study investigates fatal opioid overdoses in Riverside County, California, between January 2020 and March 2023, employing advanced spatial-temporal analysis methods to uncover significant clusters and their underlying contexts. By integrating global and local Knox tests, the research identifies both broad trends and specific hotspots of fatal overdoses. The findings reveal substantial spatial disparities, with higher overdose rates in rural areas and neighborhoods characterized by lower socioeconomic status and larger Hispanic populations. Despite a lower overall overdose risk among Hispanics, their neighborhoods exhibit a higher occurrence of fatal overdoses, highlighting complex interactions between individual and environmental factors. These insights underscore the need for targeted, contextually informed public health interventions and policies to effectively address the opioid crisis.

1 | Introduction

In the United States over the last two decades, fatal drug overdoses have increased five-fold (Spencer 2022). During the year 2021, an average of 220 people died *each day* from an opioid overdose.[1] The rise in overdose death rates at the national scale during this period, while astronomic and attention-grabbing, masks substantial variations in drug-related deaths within the country. For example, in 2021, the drug overdose mortality rate across states ran from a low of 11.4 deaths per 100,000 population in Nebraska to a high of 90.9 in West Virginia.[2]

Research into these wide spatial disparities is relatively limited (Congdon 2020).[3] This is an important gap, as from a scientific point of view, improved understanding of the individual risk factors (Altekruse et al. 2020), contextual or neighborhood effects (Delmelle and Rey 2021), and structural forces such as variation in policies towards the crisis (You et al. 2020) is critical. Moreover, these compositional and contextual dimensions may interact in complicated ways contingent on geography. There is also the potential to use the results from spatial analysis to inform the geographical targeting of interventions such as harm reduction programs.

What's more, the studies that have adopted a spatial lens on the opioid crisis vary in the choice of spatial analysis method adopted, the extent to which the dynamics of the patterns are incorporated, and the spatial scale of the investigation. Several studies employ global and local spatial autocorrelation statistics to examine the spatial pattern of overdoses across counties (Congdon 2020) as well as within particular counties (Hess and Zhang 2022) or individual municipalities (Stopka et al. (2021)), Forati et al. (2021)). The global tests address whether the spatial pattern displays clustering in overdose activity, while the local tests are used to

identify the locations of specific areas that may be driving the overall pattern.

Alongside changes in spatial scale, the treatment of the temporal dimension also varies across studies. A common approach is to aggregate data from multiple time periods into a single interval that is then analyzed using cross-sectional methods (Congdon (2020), Dworkis et al. (2017), Kolak et al. (2020)). An alternative to temporal aggregation is the repeated application of the spatial tests to each period of the analysis (Wilt (2019), Park et al. (2021)). Still, other studies focus on the issue of space-time interactions in opioid overdose activity (Mohler et al. (2021), Li et al. (2023)).

In this paper, we aim to contribute to the literature on the space-time dynamics of opioid overdoses in several ways. First, we introduce a novel approach to analyzing overdoses at the intraurban scale. This method addresses a gap in the existing literature, which predominantly uses global analytics for studying space-time patterns at the city scale (Ray et al. 2023). Our approach offers a local perspective and integrates both local and global analytics at this spatial level. Additionally, we present an alternative method for local inference.

Second, our method enables the detailed examination of the individual and contextual characteristics of space-time hotspots of fatal overdoses. This allows us to investigate disparities between different groups, such as those who are part of hotspots vs. those who are more isolated, as well as between areas with and without overdoses.

Third, we demonstrate these new methods through an empirical analysis of daily fatal opioid overdoses in Riverside, California, covering the period from January 1, 2020, to March 1, 2023.

The remainder of the paper is organized as follows: In Section 2, we outline our method for intraurban space-time analysis of opioid overdoses. Section 3 describes the dataset and context for our study. The empirical analysis, applying these methods to the case of Riverside County, California, is presented in Section 4. We discuss the implications of our findings in Section 5. We close the paper in Section 6 with a summary of theoretical contributions and practical applications, the limitations of our study, and areas for future research.

2 | Methodology

2.1 | Global Tests for Space-Time Interaction in Opioid Overdoses

The Knox test (Knox and Bartlett 1964) is a statistical method used to assess the presence of space-time clustering in a dataset. It is commonly employed in various fields, including epidemiology (Mohler et al. 2021), ecology (Dale and Fortin 2014), and criminology (Briz-Redón et al. 2022), to determine whether events or cases of interest are clustered both in space (location) and time (time periods). The Knox test helps researchers identify patterns that may indicate the presence of underlying factors or causes leading to clustering.

The Knox test is based on a count of the number of event pairs that are observed within a prespecified critical time interval τ and a prespecified critical spatial distance δ. Given n events, in our case fatal overdoses, located in space and time, there are $N = n(n-1)/2$ unique event pairs. The test focuses on the distribution of the counts of these event pairs with respect to the critical thresholds. Two overdoses are *space-time neighbors* if the pair is close in both space and time. The observed number of space-time neighbors forms the statistic.

Let N_t be a random variable representing the number of overdose pairs that are close in time relative to the specified τ. Similarly, let N_s be the random variable representing the number of overdose pairs that are close in space relative to δ. Finally, let X represent the random variable measuring the number of case pairs that are close in both space and time.

Under the null hypothesis that there is no space-time interaction in overdoses, the expected value of X is $E[X|N_s, N_t] = N_s N_t / N$. Inference on the Knox statistic can be based on one of several approaches. When N_t and N_s are small compared to N, X has been shown to be approximately Poisson distributed (Knox and Bartlett 1964). Thus, inference can be based on the Poisson assumption, with the mean of the statistic equal to its expectation.

A second alternative to inference on N_{st} uses a normal approximation to the Poisson distribution.

The third approach relies on results from Barton and David (1966), who show that the statistic N_{st} has variance:

$$V(N_{\text{st}}) = \frac{2n_s n_t}{n(n-1)} + \frac{4\nu_s \nu_t}{n(n-1)(n-2)} + \frac{4\left[n_s(n_s-1)-\nu_s\right]n_t(n_t-1-\nu_t)}{n(n-1)(n-2)(n-3)} - \left[\frac{2n_s n_t}{n(n-1)}\right]^2 \quad (1)$$

with $\nu_s = \frac{1}{2}\sum_i n_s(i)^2 - n_s$, $\nu_t = \frac{1}{2}\sum_i n_t(i)^2 - n_t$, $n_t(i)$ the number of overdoses occurring within the time window τ of overdose i, and $n_s(i)$ the number of overdoses within distance δ of overdose i. Here, a normal approximation can be employed with the mean as the expectation under the null and the variance from Equation (1).

Finally, a fourth approach to inference employs Monte Carlo methods by randomly permutating the time labels of the overdoses across the spatial coordinates of the overdoses.

2.2 | Local Space-Time Clustering

Indications of global clustering naturally lead to questions about *local* clusters of space-time interaction. Rogerson (2001) has developed a local version of the Knox statistic designed to identify those pairs of observations that are close in both space and time and to assess the statistical significance of the spatial association of the involved observations. Let $n_s(i)$ represent the number of spatial neighbors for overdose i, $n_t(i)$ be the number of overdoses that are close in time to overdose i, and $n_{\text{st}}(i)$ be the number of overdoses that are close in space and time to overdose i. The local Knox statistic $N_{\text{st}}(i)$ is equal to $n_{\text{st}}(i)$. Rogerson notes that the local

statistic satisfies the property that the global Knox statistic can be related to a proportional sum of the local statistics:

$$\sum_{i=1}^{n} n_{\text{st}}(i) = 2n_{\text{st}} \tag{2}$$

This is an important result, as to date in the opioids literature, only global applications of the Knox statistic for space-time interaction have been applied (Mohler et al. 2021). Applying the local version here allows us to consider the linkage between the global and local measures. More specifically, in cases where the global Knox is significant, the local version can provide insights into the specific observations that may be driving the space-time interaction.

Under the null hypothesis of no local space-time interaction, $N_{\text{st}}(i)$ has the distribution:

$$p(N_{\text{st}}(i) = n_{\text{st}}(i)) = \frac{1}{n} \frac{\sum_{j=1}^{n} \binom{n_t^j(i)}{n_{\text{st}}} \binom{n-1-n_t^j(i))}{n_s(i)-n_{\text{st}})}}{\binom{n-1}{n_s(i)}} \tag{3}$$

which is a weighted sum of hypergeometric distributions under the assumption of equally likely permutations of time labels. Here, $n_t^j(i)$ is the number of overdoses that are within the time window τ of overdose i when the latter is assigned the time associated with the jth most recent observation. Let $j = 1, \ldots, n$ be the ordered index of time periods assigned to location i. When $j = 1$, observation i has been assigned the time of the earliest overdose, and when $j = n$, i has been assigned the time of the last overdose.

Similar to the case of the global Knox, there are several alternative approaches to inference that have been suggested. Rogerson suggests that an exceedance probability be used:

$$p(N_{\text{st}}(i) \geq n_{\text{st}}(i)) = \sum_{k=n_{\text{st}}}^{\max_j\{n_t^j(i)\}} \frac{1}{n} \frac{\sum_{j=1}^{n} \binom{n_t^j(i)}{k} \binom{n-1-n_t^j(i))}{n_s(i)-k)}}{\binom{n-1}{n_s(i)}} \tag{4}$$

Alternatively, Rogerson also suggests a normal approximation can be used:

$$z_i = \frac{n_{\text{st}}(i) - E\{N_{\text{st}}(i)\} - 0.5}{\sqrt{V\{N_{\text{st}}(i)\}}} \tag{5}$$

with

$$E\{N_{\text{st}}(i)\} = \frac{2n_t n_s(i)}{n(n-1)} \tag{6}$$

and

$$V\{N_{\text{st}}(i)\} = \frac{\left\{2(n-1)n_t - \sum_{j=1}^{n} n_t^j(i)^2 n_s(i)\{n-1-n_s(i)\}\right\}}{n(n-1)^2(n-2)} \tag{7}$$

These two approaches are based on approximations, and this raises the question of how well these approximations hold in practice. We suggest a complementary approach based on conditional random permutations, inspired by the strategy used in the analysis of local indicators of spatial association (Anselin 1995). In contrast to the permutation strategy used to assess the significance of the global Knox, where all time labels are randomly reassigned in each permutation, the conditional permutation approach we suggest carries out a different permutation for each spatial location. More specifically, we fix the time label at the observed value for overdose i and then carry out a permutation of the remaining $n-1$ time labels over the other $n-1$ overdose locations. For each overdose, we repeat these conditional permutations to build up the reference distribution for the local space-time Knox for overdose i.

2.3 | Unpacking Space-Time Clusters

Identification of local space-time clusters of opioid overdoses raises questions about the contextual and individual factors that may be related to the locations of these hotspots and how those factors may differ between overdoses that do not belong to a cluster, as well as other locations in the region where overdoses have not occurred in the sample period.

In this section, we outline methods that can be used to address these questions. We adopt a pseudo-case-control framing that is applied in two ways. In the first application, our cases are defined as locations that had an overdose, irrespective of whether the case is a member of a hotspot. To define the context for each case, we apply a spatial buffer with radius δ to the location of the overdose. We then interpolate contextual attributes, including socioeconomic and race/ethnicity composition, into the buffers to estimate the context for each case.

To ensure that each control is separated from a case by at least δ units, we extend the buffers around each case by another δ units. Next, we form the unary union of these buffers. We then form the spatial difference between the region and this unary union. The difference is the area of the spatial extent that has been free of overdoses during the sample period and contains points that are at least δ away from any case buffer.

We then select n_{control} points within this area, with the probability of a location for a point being proportional to the population at risk. The latter is determined by the spatial interpolation of the observed population into hexagons formed from a tessellation of the area. We then buffer each of the $n_{control}$ points using a radius of δ and then interpolate the same socioeconomic and race/ethnicity variables used with the cases into these control buffers.

We then assess the statistical significance of the observed difference in an attribute between these two sets of locations (case and control locations) by carrying out 10,000 random labelings of the pooled locations and measuring the difference for each relabeling to develop the reference distribution under the null hypothesis of no difference in the attribute distributions between the case and control locations.

In this first application, we are interested in exploring whether the spatial contexts differ between locations with overdoses and those free from overdoses. In the second application, we redefine the cases as those overdoses that were part of a hotspot, and the "controls" as overdoses that are not part of a cluster. Here, we are interestedz in whether there are contextual and/or

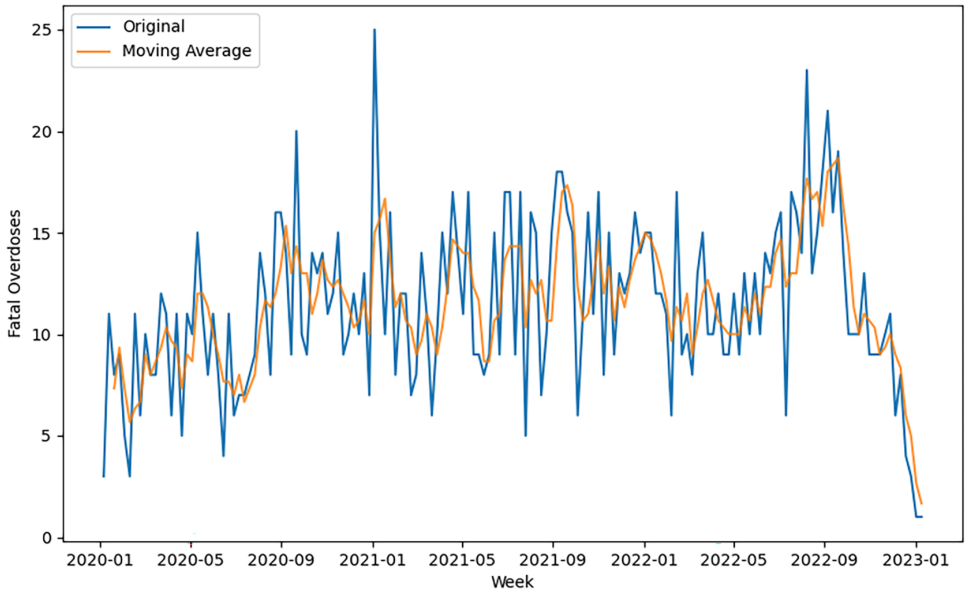

FIGURE 1 | Weekly fatal opioid overdoses, Riverside County, California, 2020-01 through 2023-01. The moving average uses a rolling 3-week window.

TABLE 1 | Excess risk factors by race/ethnicity.

	Population share	OD deaths share	Excess risk
White	0.353	0.503	1.425
Hispanic/Latino	0.489	0.338	0.691
Black or African American	0.061	0.083	1.367
Asian	0.066	0.013	0.192
American Indian or Alaska Native	0.020	0.010	0.500

individual-level factors that vary between clustered overdoses and isolated overdoses.

3 | Data Sources

We collaborated with the Riverside University Health System (RUHS), Public Health, as part of a broader partnership in research and programming to address overdose and promote harm reduction in our communities. Our analysis draws from California Death Registry Data for Riverside County overdose deaths, focusing on the International Classification of Diseases, Tenth Revision (ICD-10) Codes of X40–X44, X60–X64, X85, Y10–Y14. ICD-10 codes allow standardized classification and analysis of causes of death. The ICD considers a death to be a drug overdose death (by drugs, medications, or other substances) if any of the following ICD-10 codes is an underlying cause of death: X40–X44 (unintentional), X60–X64 (suicide), X85 (assault), and Y10–Y14 (undetermined intent). In addition, we were provided with geographic data and individual characteristics of the deceased including age, gender (the legal sex or gender identity of the decedent as on the death certificate) and race-ethnicity ("American Indian/Alaska Native," "Asian," "Black," "Hawaiian/Pacific Islander," "Hispanic," "Multi-Race," "White," and "Other/Unknown." All records with a response of "Yes" to "Was decedent Hispanic/Latino(a)/Spanish?" are included in "Hispanic" regardless of race). RUHS provided regular, secured transmissions of county-wide data; the period analyzed here covers January 2020–January 2023. We geocoded the locations based on the reported address of the injury in the registry.

4 | Results

4.1 | Fatal Overdoses in Riverside County, CA 2020-01 Through 2023-01

We begin with a descriptive analysis of the fatal opioid overdoses in the county. During our sample period, there were 1895 fatal overdoses reported. Given that our sample period covers 158 weeks, and the county population at the midpoint of this interval stood at 2.489 million, the crude rate of overdose deaths was 25.07 per 100,000 per year in the county, while the age-adjusted rate was 24.86. The latter was below the national age-adjusted rate of 28.51 in 2021.[4]

Figure 1 reports weekly overdose fatalities over the study period. The mean number of fatal overdoses per week was 11.39, with a maximum of 25 (first week of 2021), minimum of 1, and a standard deviation of 4.1.[5]

Table 1 provides summary measures of the composition of the Riverside County population, as well as the overdose distribution by ethnic and racial categories. Whites and Black populations experience excess risk, while the Hispanic, Asian, and American Indian groups have disproportionately lower overdose rates. The higher rates for the White and Black population, and the relatively lower rates for the Hispanic population in Riverside, mirror the findings at the national level for these groups (Lippold 2019).

FIGURE 2 | Riverside county, California. Census designated places in red.

Riverside County, located in Southern California, had a population of approximately 2.42 million residents in 2020. The county spans over 7300 square miles, encompassing diverse geographic features from desert landscapes to mountain ranges. As illustrated in Figure 2, the majority of the population is concentrated in the western part of the county, where cities like Riverside, Moreno Valley, and Corona form a densely populated urban corridor. This western region serves as a hub for economic activity and residential communities, contrasting sharply with the more sparsely populated eastern areas dominated by vast open spaces and natural reserves.

Figures 3 and 4 provide an overview of the spatial context of fatal opioid overdoses in Riverside County over the sample period. Figure 3a shows population density in Riverside using a regular hexagonal grid system (with data interpolated from the 2020 American Community Survey), and Figure 3b shows the level of racial integration in each location as measured by the entropy index, which ranges from a low of zero (when individuals all belong to a single racial group) to a high of one (when members are spread evenly across groups), with the latter indicating greater racial diversity. The northwest portion of Riverside County, which includes cities such as Riverside and Moreno Valley, features a higher population density due to its proximity to major metropolitan areas and better infrastructure, with the city of Riverside itself having a density of approximately 1497 people per square kilometer. In contrast, the eastern side of the county,

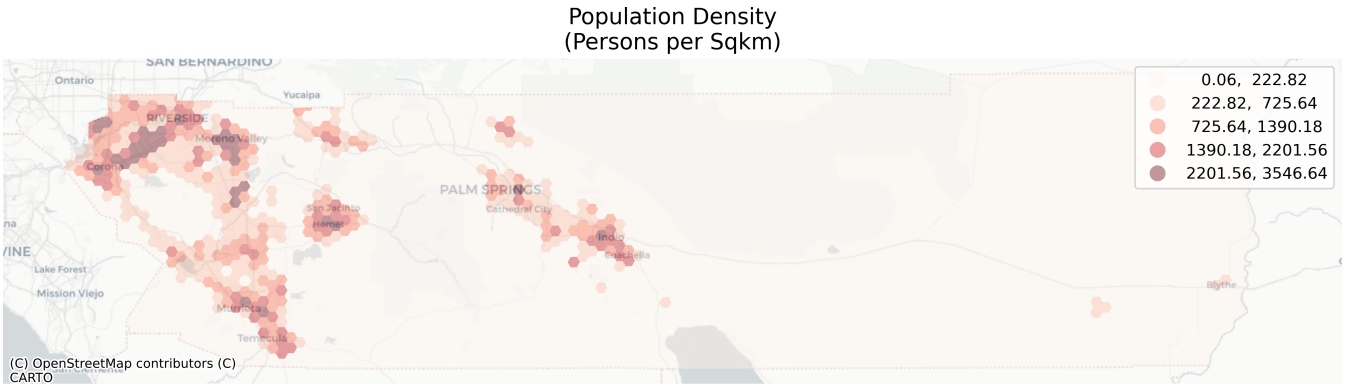

(a) Population density

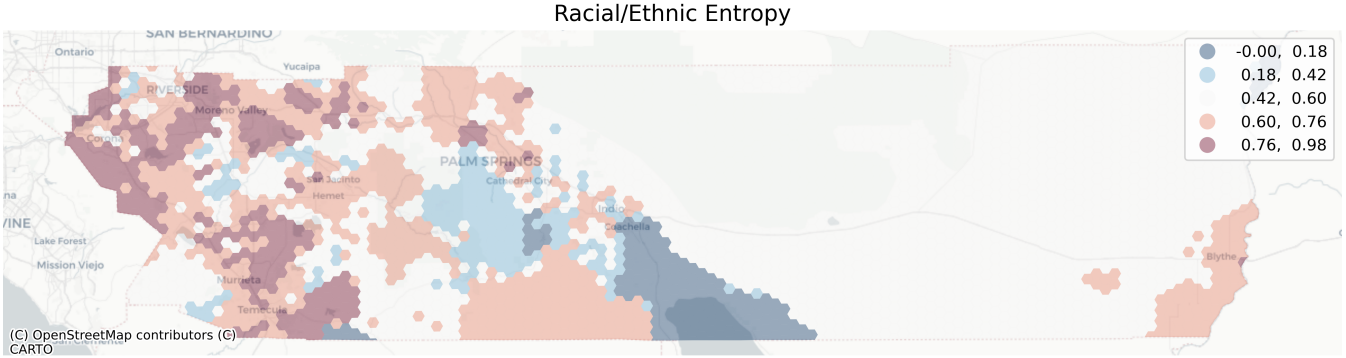

(b) race/ethnicity entropy

FIGURE 3 | Riverside county population density and race/ethnicity entropy. (a) Population density, (b) race/ethnicity entropy.

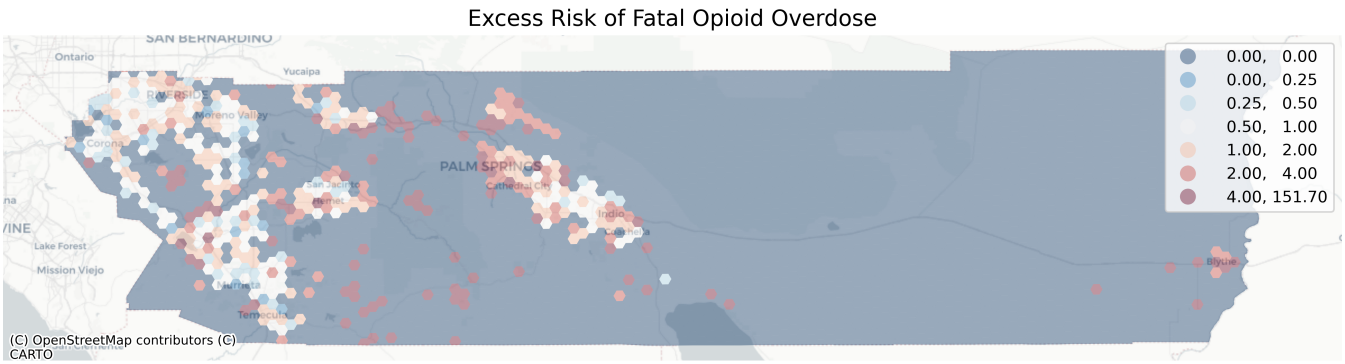

(a) Excess risk of fatal opioid overdoses

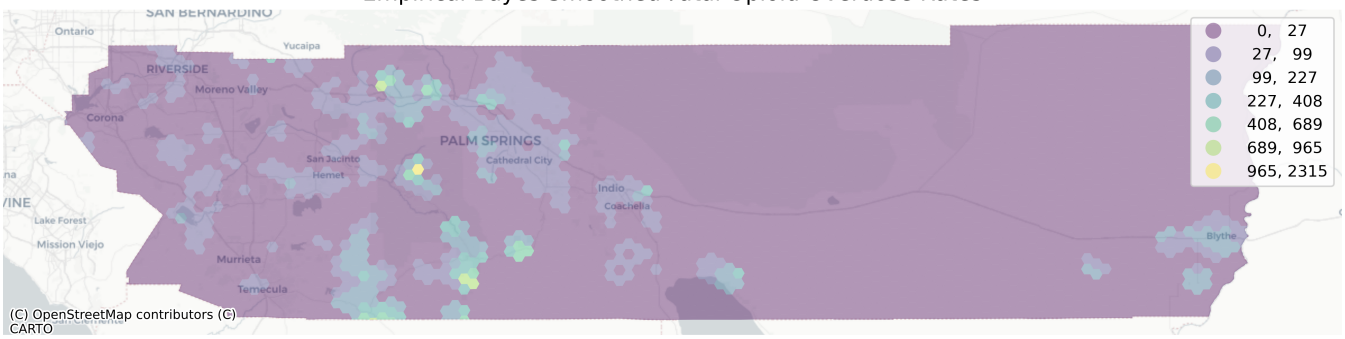

(b) Empirical Bayes smoothed fatal overdose rates (per 100000, Fisher Jenks k=7 classification)

FIGURE 4 | Riverside county fatal opioid overdoses. (a) Excess risk of fatal opioid overdoses, (b) empirical Bayes smoothed fatal overdose rates (per 100,000, Fisher Jenks $k = 7$ classification).

encompassing vast desert areas and rural communities, remains sparsely populated. More racially integrated communities tend to locate along urban cores where the entropy scores are the highest.

Turning to the spatial distribution of fatal overdoses, Figure 4a,b provides two different lenses on the spatial patterns. In both cases, we aggregate individual overdoses to standardized hexagons to protect privacy. Figure 4a maps the excess risk by grid cell. The categories for excess risk are defined using the standardized mortality rate:

$$\text{SMR}_i = \frac{O_i}{E_i} \tag{8}$$

where O_i is the number of fatal overdoses that occurred in cell i over the sample period, and E_i is the expected number of overdoses. The latter is obtained as:

$$E_i = \tilde{\Theta} \times P_i \tag{9}$$

with:

$$\tilde{\Theta} = \frac{\sum_i O_i}{\sum_i P_i} \tag{10}$$

where P_i is the population of cell i. In the excess risk map, blue hues represent grid cells where the risk is less than the county average, whereas red hues reflect grid cells having elevated risk relative to the county average. Generally, the areas where risk is in line with the county-wide average tend to be located in areas of high population density. Cells with higher levels of risk are on the edges of these areas as well as being scattered throughout the county, with a particular concentration of high excess risk cells in the extreme eastern part of the county.

Interpretation of the spatial patterns on risk maps is complicated by several statistical issues (Gelman and Price 1999). Chief among these are the instability in the counts due to the rarity of events, and the large variance in the sizes of the population at risk across the cells, which can lead to intrinsic variance instability in the risk estimates, and a resulting emphasis on units with small populations.

One approach to these sources of instability in the raw rate estimates is to apply smoothing or shrinkage estimators that borrow strength from other observations in the dataset to dampen raw estimates to mitigate spurious outliers. We adopt an empirical Bayes approach based on a Poisson-Gamma model. The observed overdose counts, O_i, are specified as draws from a Poisson distribution conditioned on the risk parameter and the population in cell i:

$$O_i \sim \text{Poisson}(P_i \cdot \Theta_i) \tag{11}$$

where Θ_i is the risk parameter for cell i. The prior for the risk parameter is a Gamma distribution:

$$\Theta_i \sim \text{Gamma}(\nu, \alpha) \tag{12}$$

with ν the shape parameter, and α the scale parameter. This distribution has a mean of ν/α and variance ν/α^2. Combining the Gamma prior for the risk parameter with a Poisson distribution for the overdose counts generates the posterior distribution of Θ_i given O_i as Gamma$(O_i + \nu, P_i + \alpha)$. The resulting mean and variance of the posterior for the risk parameter are:

$$E\left[\Theta_i | O_i\right] = \frac{\nu + O_i}{\alpha + 1} \tag{13}$$

and

$$V\left[\Theta_i | O_i\right] = \frac{\nu + O_i}{(\alpha + P_i)^2} \tag{14}$$

The smoothed Bayes estimates of Θ_i are given by:

$$\hat{\Theta}_i = w_i r_i + (1 - w_i)\gamma_i \tag{15}$$

where

$$w_i = \frac{\phi_i}{\phi_i + \gamma_i / P_i} \tag{16}$$

with $\gamma_i = \frac{\nu}{\alpha}$, and $\phi_i = \frac{\nu}{\alpha^2}$. From Equation (16), the weight will grow with the size of the population at risk in cell i, placing more weight on the observed rate for cell i. The weight is also a function of the variance of the prior distribution for the rates, ϕ_i.

To estimate the weights in Equation (16), the empirical Bayes approach assumes that the prior means for each cell are equal: $\gamma_i = \gamma$. A similar assumption is made for the prior variances: $\phi_i = \phi$. Estimates of γ and ϕ and then obtained from the data:

$$\hat{\gamma} = \frac{\sum_i O_i}{\sum_i P_i} \tag{17}$$

and

$$\hat{\phi} = \frac{\sum_i P_i (r_i - \hat{\gamma})^2}{\sum_i P_i} - \frac{\hat{\gamma}}{\overline{P}} \tag{18}$$

Substituting (17) and (18) into (16) gives:

$$\hat{w}_i = \frac{\hat{\phi}}{\hat{\phi} + \hat{\gamma}/P_i} \tag{19}$$

and the empirical Bayes estimates of the rates as:

$$\hat{\Theta}_i = \hat{\gamma} + \frac{\hat{\phi}(r_i - \hat{\gamma})}{\hat{\phi} + \hat{\gamma}/P_i} \tag{20}$$

The resulting empirical Bayes rates shown in Figure 4b adjust for the variance instability that may plague excess risk maps such as Figure 4a. The smoothing results in a clearer pattern of the spatial distribution of fatal overdoses in the county. In general terms, the areas with the higher estimated rates tend to be outside the major population areas (see Figure 3a).

While these area maps provide an overall view of the spatial structure of overdose activity, our statistical analysis that follows is based on the locations of individual overdoses and their space-time interactions.

4.2 | Global Space-Time Interactions

Figure 5 conveys the logic of the global Knox test for space-time interaction in fatal overdoses. To protect the identity of individuals, we first embed each fatal overdose as a node in a graph. In the left figure, edges are induced between pairs of overdoses that occurred within 500 meters of each other, irrespective of their dates of occurrence. This is the spatial-neighbor adjacency graph. Then, we filter the edges to include only those that are both spatial and temporal neighbors to form the graph on the right. This is the space-time neighbor graph, which connects all pairs of overdoses that occurred within 500 meters of each other and 7 days.

Table 2 summarizes the global Knox statistic results for 28 different space-time thresholds, using critical time periods of 7, 14, 21, 28, 35, 42, and 49 days, and critical spatial distances of 500, 1000, 1500, and 2000 m. The table reports the distribution of pairs of overdoses across these different space-time windows. There are a total of 17,96,460 unique pairs of overdoses in our sample.

Focusing on the first row of the table, we consider event pairs that are within 500 meters of each other. Reading across the row are the number of pairs that were also temporal neighbors for the specified threshold in that column. For example, 42 pairs of overdoses occurred within one week of each other and were separated by less than 500 meters. Extending the time window to two weeks yields 62 pairs of overdoses, three weeks, 79 pairs, and so on up to seven weeks, at which there were 184 pairs of overdoses within 500 meters. The final column reports the total number of overdose pairs that are within 500 meters, irrespective of their separation in time. Thus, we know that the 1693 overdoses that occurred within 500 meters of each other happened at least 7 weeks apart.

The question of interest is whether the observed counts of pairs at each interval depart from what would be expected under a null hypothesis of no space-time interaction in overdoses. The observed count (Obs.) of 42 space-time pairs at the 500-meter and 7-day interval exceed the expected value (Exp.), 24.7, under the null hypothesis of no space-time interaction. The significance of this difference is based on two different frameworks. The "p-poisson" value is the probability of observing 42 or more space-time pairs under the null hypothesis of space-time independence, where the count has a Poisson distribution with an expectation of 24.7. In this case, the p value of 0.01 is indicative of a significant departure from this expectation and points to space-time clustering within the 500-meter–1-week interval.

The second approach to inference is reported in the rows labeled "p-sim," where the pseudo p values are obtained by random permutation of the event times among the fixed spatial locations. Here, we repeat the permutations 99 times, recalculating the global Knox statistic for each resulting permutation. Collecting these statistics across the permutations provides a computationally based reference distribution for the global statistic under the null hypothesis of no space-time interaction. The p value is obtained as:

$$p\text{-sim} = \frac{1 + \sum_{r=1}^{99} I(\text{knox}_r >= 42)}{1 + 99}$$

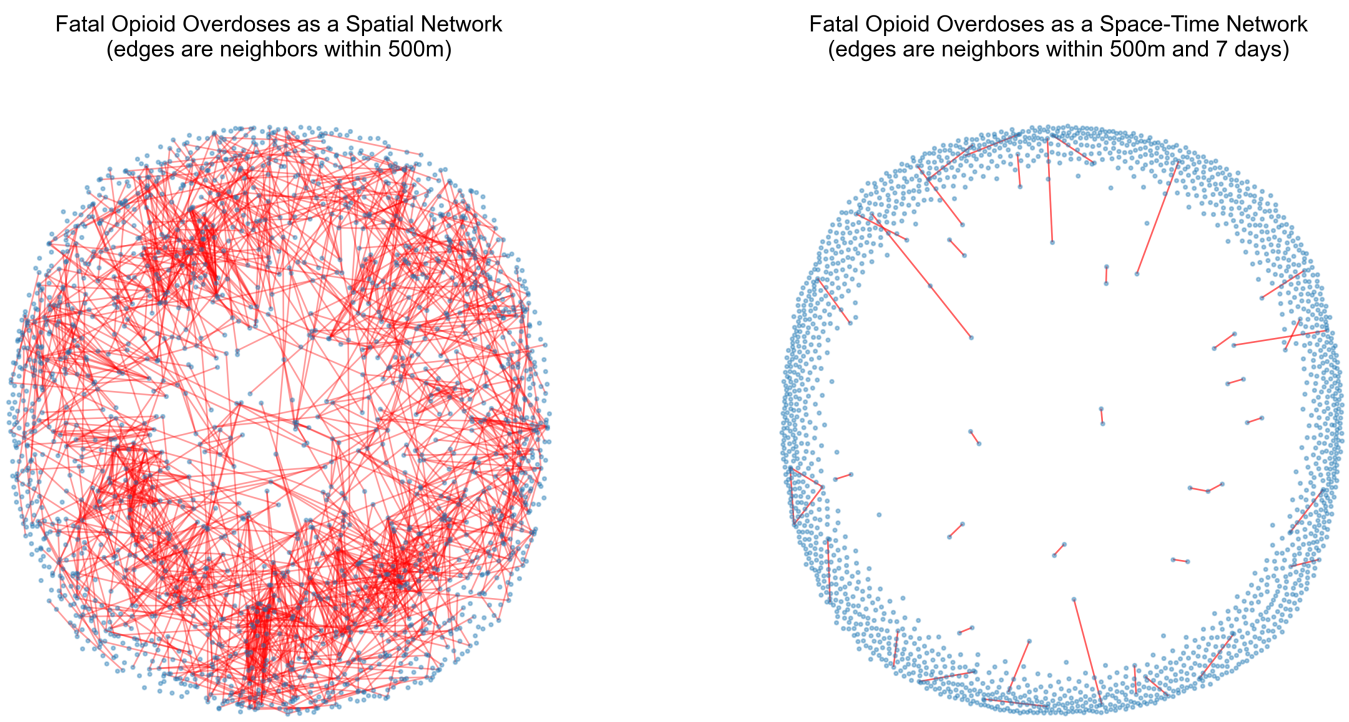

FIGURE 5 | Random embedding of spatial neighbor graph (left) and space-time neighbor graph (right) fatal overdose, Riverside County, California, 2020-01 through 2023-01.

TABLE 2 | Global knox tests for space-time interactions.

Distance	Count	< 7	< 14	< 21	< 28	< 35	< 42	< 49	Total
< 500	Obs.	42	62	79	118	135	163	184	1877
	Exp.	24.7	48.0	71.3	94.5	117.4	140.3	163.0	
	p-poisson	0.00	0.02	0.17	0.01	0.05	0.03	0.05	
	p-sim	0.01	0.03	0.22	0.03	0.07	0.05	0.08	
<1000	Obs.	91	152	217	300	353	423	490	5712
	Exp.	75.1	146.2	217.0	287.6	357.3	426.8	495.9	
	p-poisson	0.03	0.30	0.48	0.22	0.58	0.56	0.59	
	p-sim	0.04	0.39	0.53	0.19	0.60	0.59	0.67	
< 1500	Obs.	143	278	405	551	673	823	948	10,809
	Exp.	142.2	276.7	410.6	544.3	676.0	807.7	938.4	
	p-poisson	0.45	0.45	0.60	0.38	0.54	0.29	0.37	
	p-sim	0.59	0.38	0.62	0.48	0.55	0.30	0.42	
< 2000	Obs.	233	444	650	866	1055	1296	1495	17,021
	Exp.	223.9	435.6	646.6	857.1	1064.6	1271.8	1477.8	
	p-poisson	0.26	0.33	0.44	0.37	0.61	0.24	0.32	
	p-sim	0.31	0.35	0.45	0.38	0.60	0.29	0.29	
Total		23,631	45,980	68,244	90,460	112,358	134,233	155,970	1,796,460

where $I(\text{knox}_r >= 42)$ is a binary indicator function signaling if the value for the global statistic from permutation r was as extreme as the observed value. For this first interval (500,7), the permutation-based inference agrees with the analytical approach, again pointing to significant space-time interaction at that interval. In general, the simulation-based approach is more conservative across intervals, reflected in the larger p value at each space-time window.

There is strong evidence of space-time interaction at the spatial scale of 500 meters, as both approaches to inference yield significantly higher counts than expected for all but a single time interval (3 weeks). Moreover, as the spatial threshold increases beyond 500 meters, the observed counts cannot be viewed as significant departures from randomness. The one exception is the 1000-meter, 7-day interval, where significant interaction is detected.

TABLE 3 | Space-time hotspots of fatal opioid overdoses. A "—" in the p value column indicates the overdose is a member, but not a core of a hotspot.

Cluster	Overdose	p	Day	Neighbor	Orientation
0	420	—	223	445	Lead
0	445	0.05	230	420	Lag
1	506	0.04	255	517	Lead
1	517	0.02	257	506	Lag
1	522	0.03	259	506	Lag
2	671	0.03	319	672	Coincident
2	672	0.04	319	671	Coincident
3	832	0.05	393	833	Coincident
3	833	0.03	393	832	Coincident
4	905	0.03	427	908	Lead
4	908	0.01	431	905	Lag
5	938	0.05	443	922	Lag
5	922	0.02	436	938	Lead
6	933	0.01	441	932	Coincident
6	932	0.01	441	933	Coincident
7	946	0.03	448	947	Lead
7	947	—	449	946	Lag
8	1243	0.04	562	1256	Lead
8	1256	0.04	566	1243	Lag
9	1266	0.03	568	1248	Lag
9	1248	—	563	1266	Lead
9	1276	—	571	1266	Lag
10	1251	0.02	564	1261	Lead
10	1261	0.02	567	1251	Lag
11	1425	0.03	624	1419	Lag
11	1419	0.02	623	1425	Lead
12	1608	0.04	703	1616	Lead
12	1616	—	706	1608	Lag
13	1641	0.05	716	1648	Lead
13	1648	—	717	1641	Lag
14	1657	0.05	722	1658	Coincident
14	1658	0.02	722	1657	Coincident
15	1750	0.02	751	1751	Coincident
15	1751	0.04	751	1750	Coincident
16	1819	—	780	1816	Coincident
16	1816	0.04	780	1819	Coincident
17	1841	0.01	791	1839	Coincident
17	1839	0.01	791	1841	Coincident
18	2227	0.02	938	2237	Lead
18	2237	0.01	941	2227	Lag
19	2302	0.03	961	2310	Lead
19	2310	0.04	963	2302	Lag
20	2320	—	966	2321	Coincident
20	2321	0.01	966	2320	Coincident
20	2323	—	967	2321	Lag
21	2505	—	1027	2530	Lead
21	2530	0.05	1034	2505	Lag
22	2610	—	1081	2599	Lag
22	2599	0.02	1074	2610	Lead
23	2609	0.02	1080	2710	Coincident
23	2710	0.01	1080	2609	Coincident

4.3 | Local Space-Time Clusters

Given the strong evidence of global space-time interaction across the different time intervals within the 500-meter spatial radius, we turn to the application of the Local Knox statistic to identify individual locations that have local space-time association that is stronger than what would be expected under the null hypothesis of space-time randomness.

We define a space-time hotspot as a subgraph induced on the global space-time graph where the edges connect a focal overdose with a significant Local Knox statistic to its space-time neighbors. Table 3 reports 24 such hotspots when $\tau = 7$ and $\delta = 500$. Focusing on hotspot 1, three overdoses form the nodes of this subgraph (506, 517, 522). For overdose with ID 506, its space-time neighbors are overdoses 517 and 522. We also see that this focal overdose preceded the neighboring overdoses by 2 and 4 days, respectively.[6]

This hotspot is differentiated from hotspot 0; the latter involves focal overdose 420 and space-time neighbor 445. For hotspot 0, the number of space-time neighbors for observation 445 is a significant departure from what would be expected under the local null, while for observation 420, its number of space-time neighbors does not depart from randomness. Thus, in this case, the hotspot involves two overdoses, only one of which has a significant Local Knox statistic. In contrast, for hotspot 1, three overdoses are involved, each of which has significant Local Knox statistics, albeit with different numbers of observed space-time neighbors.

Of the 24 overdose hotspots, 21 involve pairs of overdoses, and three consist of triples of overdoses. Nine of the hotspots involved fatal overdoses on the same day (temporally coincident). Of these nine hotspots, eight involved pairs of overdoses that were also spatially coincident (same address), while one of the nine hotspots had temporally coincident overdoses occurring at three different, nearby addresses.

4.4 | The Residential Context of Fatal Overdoses

The presence of significant space-time interaction among fatal opioid overdoses suggest there may be important differences in the places (or times) that fatal overdoses occur. In other words,

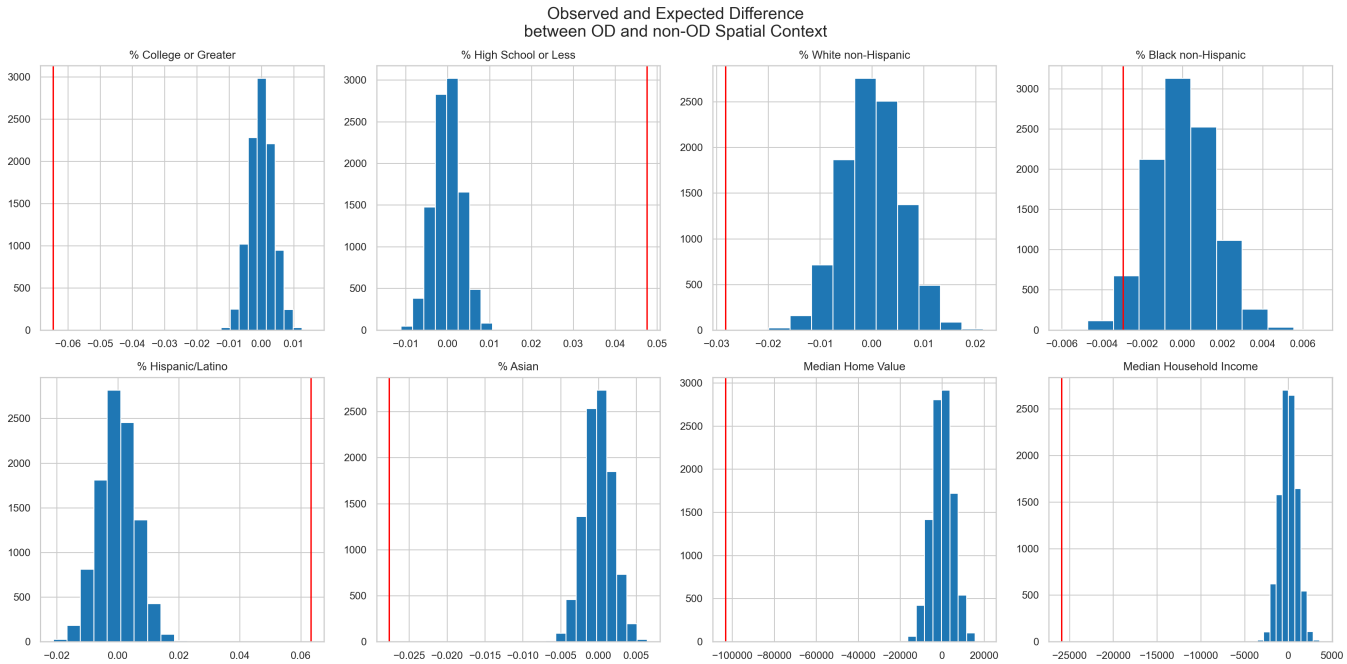

FIGURE 6 | Comparing spatial contexts between locations with fatal overdoses and locations free from overdoses.

given the evidence of significant clustering, there may be differences in the urban fabric or demographic makeup of the places where overdoses occur. We test for these potential differences as follows. Adopting the computational inference strategy described in the Section 2.3, we first compare the spatial contexts of each overdose (defined by a buffer of distance δ, here 500 meters) versus a simulated control group.

These tests show clear differences, both substantive and statistical, between the spatial contexts where overdoses are observed and those contexts where they are not. In general, the patterns show that fatal overdoses are observed significantly more often in neighborhoods with lower incomes, lower housing values, and lower educational attainment. The patterns all mirror the populations among whom overdoses themselves are more prevalent (i.e., where the concentration quotient is greater than one), which may suggest some structural inequality between high socioeconomic status (SES) and low-SES residents in Riverside County, where the risk of fatal overdoses appears significantly greater among both lower-income and lower-educated groups, *and* lower-income and lower-educated neighborhoods.

The graphs in Figure 6 show these comparisons for each variable; the red vertical line shows the observed difference, on average, between the fatal overdose contexts, and the blue histogram displays the distribution of synthetic differences drawn from 10,000 random reassignments of the overdose versus non-overdose location labels. Pseudo p values associated with each observed difference are shown in Table 4, however, the graphic conveys this "significance" clearly in cases where the red bar is obviously outside the blue histogram (i.e., outside the typical distribution). Every variable tested shows a significant difference between contexts, except for the share of the non-Hispanic Black population. This means that, on average, the characteristics of the neighborhoods where fatal overdoses occurred were statistically different from a set of synthetic control observations that serve as a reference.

TABLE 4 | Mean difference between observed neighborhood variables and simulated null distribution for OD versus non-OD contexts.

	$\delta_{obs-exp}$	Pseudo p
Median-home-value	−103,422.473	0.000
Median-household-income	−25,395.365	0.000
p-college	−0.064	0.000
p-hsless	0.049	0.000
p-white	−0.030	0.000
p-black	−0.002	0.129
p-hisp	0.064	0.000
p-asian	−0.027	0.000

Unlike the socioeconomic variables, the results for racial composition in spatial context, highlight a stark difference. Here, the findings for spatial context contrasts with the findings from populations where fatal overdoses are more prevalent. Specifically, whereas Riverside County's white population is over-represented in the share of residents experiencing a fatal overdose, the *places* where fatal overdoses occur are significantly less non-Hispanic white than the set of synthetic controls (albeit by a very small margin). Further, the Hispanic/Latino population is underrepresented among fatal overdoses, but the locations where overdoses are roughly six percent more Hispanic/Latino in residential composition. In plain terms, fatal overdoses are significantly

more likely in neighborhoods with a larger Hispanic/Latino population, even though fatal overdoses are significantly less likely within the Hispanic/Latino population.

4.5 | The Residential Context of Fatal Overdose Space-Time Hotspots

Following, we also compare the differences between fatal overdoses that belong to a space-time hotspot against those that do not. In this comparison, many of the same patterns are prevalent as in the analysis above, but only the median household income represents a significant departure from what is expected under the null hypothesis of no differences between incomes in the two contexts. To use a regression metaphor, if each of the tested variables were treated as coefficients in a model, the signs for each coefficient would be the same, but the hotspot versus non-hotspot comparison yields smaller magnitudes and only a single significant result. These are shown in Table 5 and graphically in Figure 7.

TABLE 5 | Mean difference between observed neighborhood variables and simulated null distribution for clustered and non-clustered ODs.

	$\delta_{obs-exp}$	Pseudo p
Median-home-value	−14,628.459	0.531
Median-household-income	−10,204.920	0.021
p-college	−0.018	0.300
p-hsless	0.018	0.296
p-white	−0.016	0.594
p-black	−0.004	0.595
p-hisp	0.026	0.412
p-asian	−0.008	0.329

5 | Discussion

The results from multiple spatial analyses conducted above reveal several noteworthy patterns highlighting particular inequalities both over space and within groups. Three results, in particular, warrant further discussion; first, the pattern of fatal overdoses in Riverside County shows significant evidence of space-time clustering, suggesting that the landscape of fatal overdoses is not the result of a random process. Second, the locations where fatal overdoses occur are statistically distinct from the neighborhood contexts experienced by a simulated control group, suggesting a strong influence of socioeconomic and race/ethnicity factors that influence the occurrence of fatal overdoses. Finally, population groups in Riverside County defined by race, ethnicity, and education have differential rates of empirical risk for fatal overdoses, with white populations having greater than expected risk rates and Hispanic populations having lower than expected risk rates.

Turning first to the excess risk and empirical Bayes smoother maps shown in Figure 4a,b, the visualizations show disproportionately high risks in rural areas after accounting for the population at risk. Despite being less populated, many areas of extremely heightened risk appear in cities in Riverside County's rural Eastern portions, such as Desert Hot Springs, Banning, Indio, and Blythe. In contrast, the more populated cities like Corona and the City of Riverside have comparatively lower risk. From the perspective of harm reduction, these findings speak to the importance of coverage in not only urban areas but in the vast and rural stretches where the need is greatest.

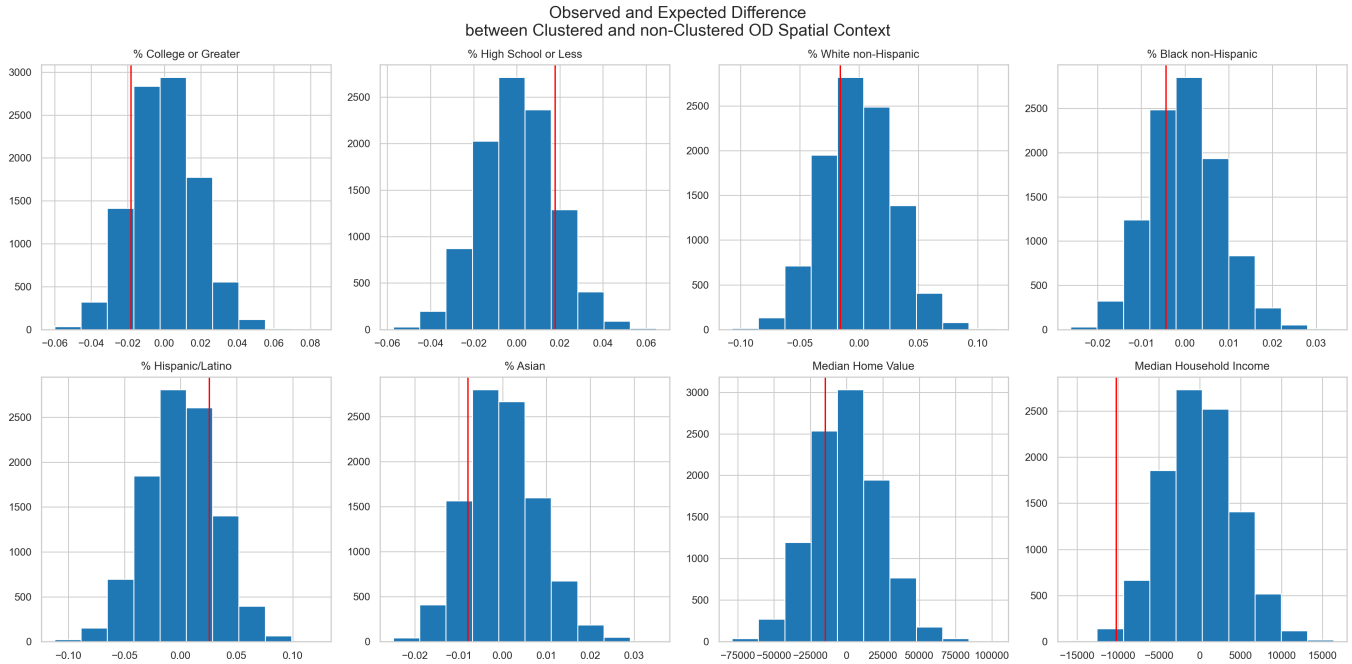

FIGURE 7 | Comparing spatial contexts between locations with overdose hotspots and locations with isolated overdoses.

In 2020, the city of Riverside gained the county's first authorized harm reduction program, which provides overdose education and naloxone distribution, and more recently, a second organization also opened. This may help explain the lower risk here and in the neighboring city of Corona. In the western region of the County, a third program operates in Palm Springs, but does not reach the smaller towns or outlying desert areas where our models have identified the greatest risk for overdose. Our results suggest that service provision models appropriate for rural areas, such as mobile harm reduction outreach, while requiring considerable investment, are also likely to have a significant impact on reducing overdose deaths.

Another prominent finding pertains to the racial and ethnic disparities—and especially their contrast—within the spatial context of fatal overdoses and the populations among whom fatal overdoses are most prevalent. More specifically, the results above show that fatal overdoses in Riverside County occur in neighborhoods that have statistically lower educational attainment, lower income populations, lower home values, and larger shares of Hispanic residents. While the prevalence of fatal overdoses in lower-income and lower-educated communities mirrors many of the inequalities faced by these neighborhoods already (including the population at risk), the fact that fatal overdoses occur in neighborhoods that are significantly more Hispanic contrasts sharply with the finding that this population has *significantly lower* risk of experiencing a fatal overdose. Many factors could be underlying this outcome, and other researchers have found that Hispanic populations in California actually had a higher risk for overdose, though rates also varied by geographic region of the state (Valdez et al. 2022). Regardless, the imbalance between *who* is at risk to overdose and *where* the risk of occurrence is greater highlights a particular disparity worthy of further inquiry—particularly understanding on-the-ground perspectives, living conditions, and access to resources across diverse communities.

From a harm reduction standpoint, we believe these results provide ample evidence that lower-resource communities (e.g., lower educational attainment and incomes) should be prioritized for outreach, however, the ramifications for racial and ethnic disparities are less clear. Overall, outreach to disadvantaged communities should be prioritized, including education, increased access to reversal medications and bystander response training, and lower medical response times would be effective since these places experience greater risk of overdose occurrence.

6 | Conclusion

The findings of our study on the space-time dynamics of opioid overdoses in Riverside County, California, highlights the crucial role of localized and temporally specific factors in understanding the patterns of fatal opioid overdoses. The utilization of advanced spatial-temporal analysis methods, including the global and local Knox tests, has allowed us to uncover significant clusters of overdose incidents and provided insights into the social, economic, and geographic contexts within which these clusters occur.

Our study confirms the presence of significant space-time clustering of opioid overdoses in Riverside County, which is reflected in other recent research (Ray et al. 2023, Sauer and Stewart 2023). This clustering suggests that certain areas experience a higher incidence of overdoses within short time frames. These clusters highlight the importance of temporal and spatial proximity in understanding overdose risks, which can inform intervention strategies.

The introduction of a local inference strategy represents an advancement in the study of opioid overdoses. Unlike previous methods that only assessed global space-time clustering, our approach uses a localized version of the Knox statistic to identify specific space-time clusters. This method involves a new conditional permutation tests that provide a detailed assessment of local interactions, improving upon traditional random permutation strategies. These advancements allow for a more precise determination of where and when overdoses are likely to cluster, which could facilitate effective outreach and interventions that are responsive to real-time data.

Our analysis demonstrates that while global spatial analyses can identify general trends, local analyses are crucial for pinpointing specific areas and times when intervention could be most effective. For example, the identification of local space-time clusters allows for a more precise understanding of where and when overdoses are most likely to occur, thus enabling more efficient allocation of resources, such as naloxone distribution and harm reduction programs tailored to community contexts.

The spatial context analysis reveals that overdoses are more prevalent in neighborhoods characterized by lower income, lower educational attainment, and higher proportions of minority populations. This aligns with broader socioeconomic research indicating that social and economic disadvantages are significant risk factors for substance abuse and related negative health outcomes. Addressing these root causes through community-based efforts, including economic and social support, education, and public health interventions, may help mitigate the risk of overdoses in these areas.

Interestingly, the places where fatal overdoses occur are less reflective of the overall demographic distribution of overdose victims. Specifically, fatal overdoses are more likely in neighborhoods with a higher proportion of Hispanic residents, despite the overall lower overdose rates among the Hispanic population. This suggests a complex interaction between individual and environmental factors that warrants further investigation to develop culturally and contextually appropriate interventions.

The insights gained from this study have direct implications for public health policy and intervention strategies. Identifying space-time hotspots can inform the placement of prevention and treatment services, such as supervised consumption sites and outreach programs, in areas with the highest need. Additionally, the findings underscore the importance of flexible and dynamic responses that can quickly adapt to emerging clusters of overdose incidents.

While this study provides valuable insights, several limitations should be acknowledged. The focus on Riverside County, California, means the findings may not be directly generalizable to other regions with different demographic and socioeconomic profiles.

However, as a geographically large and populous county (the 4th largest population in the US) with racial, socioeconomic, and infrastructural diversity, we are confident that our analysis lends valuable insights applicable to other regions. Future research should consider replicating this study in diverse settings to validate the findings and explore regional differences in overdose dynamics.

Furthermore, the study primarily relies on spatial and temporal data without extensive integration of qualitative data or contextual factors beyond basic socioeconomic indicators. Future research could benefit from a more holistic approach that includes ethnographic and qualitative data, including community perspectives and individual experiences, to enrich the understanding of the local contexts of opioid overdoses.

The application of space-time analysis methods in this study has provided a deeper understanding of the patterns and contexts of opioid overdoses in Riverside County. The evidence of significant clustering and the identification of specific high-risk areas underscore the need for focused and timely interventions to address the opioid crisis effectively. By focusing on the local nuances of overdose incidents, public health officials, policymakers, and community-based organizations can develop tailored and impactful strategies to reduce the prevalence of fatal overdoses and improve community health outcomes. The findings of this study highlight the critical importance of a spatial-temporal perspective in addressing complex public health challenges and paving the way for future research and action in this area.

Endnotes

[1] https://www.cdc.gov/opioids/basics/epidemic.html.

[2] https://www.cdc.gov/nchs/pressroom/sosmap/drug_poisoning_mortality/drug_poisoning.htm.

[3] For a recent overview see (Sauer and Stewart 2023).

[4] For Riverside County, the age-adjusted rate was determined using direct standardization with the US standard million population aggregated to 18 age cohorts in the coroner's report, together with the Riverside County age-cohort overdose mortality rates. The US age-adjusted rate is reported in https://www.cdc.gov/drugoverdose/deaths/index.html.

[5] The decline in overdoses towards the end of our sample needs to be interpreted with caution, as part of the decline may reflect the delay in the official death reporting, which would introduce an undercount at the time of our analysis, as well as a secular decline.

[6] A referee raised the concern of potential issues related to multiple comparisons when conducting local tests in spatial analysis, such as the Local Knox test used in this study. While adjustments for multiple comparisons, like the Bonferroni correction, are often employed in statistical analysis to mitigate false positives, we chose not to apply such adjustments here for several reasons. First, the nature of our research aims to explore localized spatial-temporal interactions, and applying a stringent correction may obscure meaningful spatial patterns by inflating Type II error rates. Second, the use of permutation-based inference in our approach inherently controls for randomness by constructing a null distribution specific to each observation. This allows for a more nuanced evaluation of local significance without the need for additional corrections. Finally, spatial clustering inherently implies interdependence among observations, making the assumption of independence underlying traditional multiple comparison adjustments less applicable in this context. Thus, our approach balances the need for local specificity with robust inferential methods tailored to the spatial data structure.

References

Altekruse, S. F., C. M. Cosgrove, W. C. Altekruse, R. A. Jenkins, and C. Blanco. 2020. "Socioeconomic Risk Factors for Fatal Opioid Overdoses in the United States: Findings From the Mortality Disparities in American Communities Study (MDAC)." *PLoS One* 15, no. 1: e0227966. https://doi.org/10.1371/journal.pone.0227966.

Anselin, L. 1995. "Local Indicators of Spatial Association-LISA." *Geographical Analysis* 27, no. 2: 93–115.

Barton, D., and F. David. 1966. "The Random Intersection of Two Graphs." In *Research Papers in Statistics: Festschrift for J. Neyman*, 440–459. Wiley.

Briz-Redón, Á., F. Martínez-Ruiz, and F. Montes. 2022. "Adjusting the Knox Test by Accounting for Spatio-Temporal Crime Risk Heterogeneity to Analyse Near-Repeats." *European Journal of Criminology* 19, no. 4: 586–611. https://doi.org/10.1177/1477370820905106.

Congdon, P. 2020. "Geographical Aspects of Recent Trends in Drug-Related Deaths, With a Focus on Intra-National Contextual Variation." *International Journal of Environmental Research and Public Health* 17, no. 21: 8081. https://doi.org/10.3390/ijerph17218081.

Dale, M. R. T., and M.-J. Fortin. 2014. *Spatial Analysis: A Guide for Ecologists*. 2nd ed. Cambridge University Press.

Delmelle, E. C., and S. J. Rey. 2021. "Neighborhood Effects and Neighborhood Dynamics." *Geographical Analysis* 53, no. 2: 167–169. https://doi.org/10.1111/gean.12280.

Dworkis, D. A., L. A. Taylor, D. A. Peak, and B. Bearnot. 2017. "Geospatial Analysis of Emergency Department Visits for Targeting Community-Based Responses to the Opioid Epidemic." *PLoS One* 12, no. 3: e0175115. https://doi.org/10.1371/journal.pone.0175115.

Forati, A. M., R. Ghose, and J. R. Mantsch. 2021. "Examining Opioid Overdose Deaths Across Communities Defined by Racial Composition: A Multiscale Geographically Weighted Regression Approach." *Journal of Urban Health* 98, no. 4: 551–562. https://doi.org/10.1007/s11524-021-00554-x.

Gelman, A., and P. N. Price. 1999. "All Maps of Parameter Estimates are Misleading." *Statistics in Medicine* 18, no. 23: 3221–3234. https://doi.org/10.1002/(SICI)1097-0258(19991215)18:23<3221::AID-SIM312>3.0.CO;2-M.

Hess, G. S., and C. H. Zhang. 2022. "Clustering Patterns and Hot Spots of Opioid Overdoses in Louisville, Kentucky: A Spatial Analysis of the Opioid Epidemic." *International Journal of Applied Geospatial Research (IJAGR)* 13, no. 1: 1–15. https://doi.org/10.4018/IJAGR.298303.

Knox, E. G., and M. S. Bartlett. 1964. "The Detection of Space-Time Interactions." *Journal of the Royal Statistical Society. Series C, Applied Statistics* 13, no. 1: 25–30. https://doi.org/10.2307/2985220.

Kolak, M. A., Y.-T. Chen, S. Joyce, et al. 2020. "Rural Risk Environments, Opioid-Related Overdose, and Infectious Diseases: A Multidimensional, Spatial Perspective." *International Journal on Drug Policy* 85: 102727. https://doi.org/10.1016/j.drugpo.2020.102727.

Li, Y., H. J. Miller, A. Hyder, and P. Jia. 2023. "Understanding the Spatiotemporal Evolution of Opioid Overdose Events Using a Regionalized Sequence Alignment Analysis." *Social Science & Medicine* 334: 116188. https://doi.org/10.1016/j.socscimed.2023.116188.

Lippold, K. M. 2019. "Racial/Ethnic and Age Group Differences in Opioid and Synthetic Opioid–Involved Overdose Deaths Among Adults Aged ≥18 Years in Metropolitan Areas - United States, 2015–2017." *MMWR. Morbidity and Mortality Weekly Report* 68: 967–973. https://doi.org/10.15585/mmwr.mm6843a3.

Mohler, G., S. Mishra, B. Ray, et al. 2021. "A Modified Two-Process Knox Test for Investigating the Relationship Between Law Enforcement Opioid Seizures and Overdoses." *Proceedings of the Royal Society A: Mathematical, Physical and Engineering Sciences* 477, no. 2250: 20210195. https://doi.org/10.1098/rspa.2021.0195.

Park, C., J. R. Clemenceau, A. Seballos, et al. 2021. "A Spatiotemporal Analysis of Opioid Poisoning Mortality in Ohio From 2010 to 2016." *Scientific Reports* 11, no. 1: 4692. https://doi.org/10.1038/s41598-021-83544-y.

Ray, B., S. J. Korzeniewski, G. Mohler, et al. 2023. "Spatiotemporal Analysis Exploring the Effect of Law Enforcement Drug Market Disruptions on Overdose, Indianapolis, Indiana, 2020–2021." *American Journal of Public Health* 113, no. 7: 750–758. https://doi.org/10.2105/AJPH.2023.307291.

Rogerson, P. A. 2001. "Monitoring Point Patterns for the Development of Space–Time Clusters." *Journal of the Royal Statistical Society: Series A (Statistics in Society)* 164, no. 1: 87–96. https://doi.org/10.1111/1467-985X.00188.

Sauer, J., and K. Stewart. 2023. "Geographic Information Science and the United States Opioid Overdose Crisis: A Scoping Review of Methods, Scales, and Application Areas." *Social Science & Medicine* 317: 115525. https://doi.org/10.1016/j.socscimed.2022.115525.

Spencer, M. R. 2022. *Drug Overdose Deaths in the United States, 2001–202 (CHS Data Brief, no 457)*. National Center for Health Statistics.

Stopka, T. J., E. Jacque, J. Kelley, L. Emond, K. Vigroux, and W. R. Palacios. 2021. "Examining the Spatial Risk Environmenttied to the Opioid Crisis Through a Unique Public Health, EMS, and Academic Research Collaborative: Lowell, Massachusetts, 2008–2018." *Preventive Medicine Reports* 24: 101591. https://doi.org/10.1016/j.pmedr.2021.101591.

Valdez, A., A. Cepeda, J. Frankeberger, and K. M. Nowotny. 2022. "The Opioid Epidemic Among the Latino Population in California." *Drug and Alcohol Dependence Reports* 2: 100029. https://doi.org/10.1016/j.dadr.2022.100029.

Wilt, G. E. 2019. "A Spatial Exploration of Changes in Drug Overdose Mortality in the United States, 2000–2016." *Preventing Chronic Disease* 16: 180405. https://doi.org/10.5888/pcd16.180405.

You, H.-S., J. Ha, C.-Y. Kang, et al. 2020. "Regional Variation in States' Naloxone Accessibility Laws in Association With Opioid Overdose Death Rates-Observational Study (STROBE Compliant)." *Medicine* 99, no. 22: e20033. https://doi.org/10.1097/MD.0000000000020033.